J. Phys. B: Atom. Molec. Phys. **13** (1980) 1481–1490. Printed in Great Britain

Total cross section measurements for electron scattering from molecular hydrogen at very low energies

J Ferch, W Raith and K Schröder

Fakultät für Physik, Universität Bielefeld, D-4800 Bielefeld, West Germany

Received 24 September 1979, in final form 5 November 1979

Abstract. Absolute cross sections were determined from transmission measurements made with an electron time-of-flight spectrometer in the energy range of 0·02–2 eV. The total cross section for molecular hydrogen was found to increase monotonically with energy; no resonance-like structures were observed. The isotopes H_2, D_2 and HD have identical cross sections within the accuracy of the measurements (±2·5%). Helium cross section measurements were also made in order to check the spectrometer.

1. Introduction

The motivation for studying e–H_2 scattering at very low energies came from indications that there might be resonances below 100 meV, presumably related to rotational excitations (Kouri *et al* 1969). Such resonances were discussed as an explanation for intriguing results obtained in swarm experiments (Frommhold 1968, Crompton and Robertson 1971) and indicated by structures seen in the very first e–H_2 measurements with this time-of-flight spectrometer (Land and Raith 1973).

Theoretically, these resonances appeared to be rather suspect. Molecular-orbital theory cannot account for the existence of low-lying compound states of H_2^- (Taylor and Harris 1963). The close-coupling calculations of Henry and Lane (1969) for the e–H_2 scattering did not exhibit any resonances although even a missed resonance hidden between the calculated points should have caused a noticeable phase shift. Garrett (1977) analysed rotational Feshbach-type resonances and concluded that an isolated H_2 molecule will not sustain such resonances in scattering of electrons at very low energies. Matzusawa (1975) pointed out that there is a theoretical connection between the scattering behaviour of free low-energy electrons and the weakly-bound electrons of highly excited atoms, and that old published data on spectroscopic line broadening do not support the assumption of resonances.

The cross section measurements reported here were made with an electron time-of-flight (TOF) spectrometer which was originally developed by Land and Raith (1974) at Yale University, later transferred to the University of Bielefeld, and considerably modified during the course of this work. The spectrometer now permits us to measure the energy dependence of the cross section over a wide range of energy by splicing many data sets, each obtained in a smaller energy interval. Also, absolute cross section values can now be determined.

The results presented in this paper on the e–H_2 total scattering cross section are in satisfactory agreement with the measurements of Ramsauer and Kollath (1930) as well as Golden *et al* (1966) which start at about 0·16 and 0·24 eV respectively.

0022-3700/80/071481+10$01.50

2. Apparatus

2.1. Layout

The experimental arrangement is shown in figure 1. A DC beam of 200 eV electrons is gated by RF sweeping across a narrow aperture. With an RF of 150–300 kHz the beam bursts so produced have a time width of about 7 ns. A time-distribution measurement of the primary-beam bursts is shown in figure 2. At the entrance of the drift tube, which also serves as the gas cell target, the electrons are decelerated to very low energies. At the drift-tube exit the electrons are re-accelerated to 200 eV and detected by a channel electron multiplier.

A block diagram of the electronic instrumentation is shown in figure 3. The rate of detected electrons (typically a few thousand per second) is much smaller than the burst frequency, thus the probability of more than one electron per burst reaching the detector is negligible. The electron flight time accrued while traversing the drift tube is equal to the time between the gate pulse and the electron-detection signal minus the constant flight time of the 200 eV electrons between the gate and the drift-tube entrance as well as the drift-tube exit and detector, minus the electronic delay times.

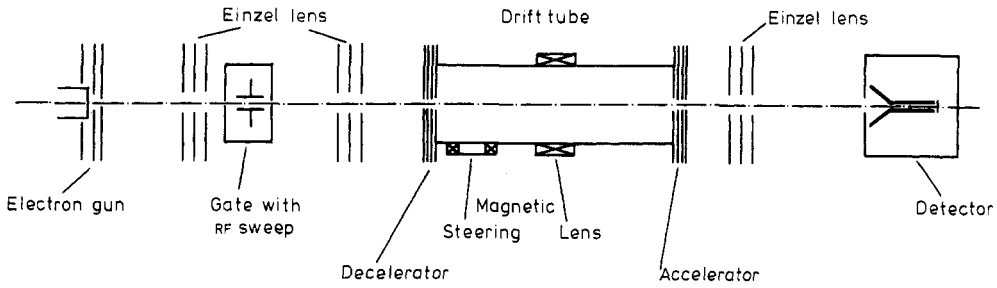

Figure 1. Experimental arrangement (not to scale).

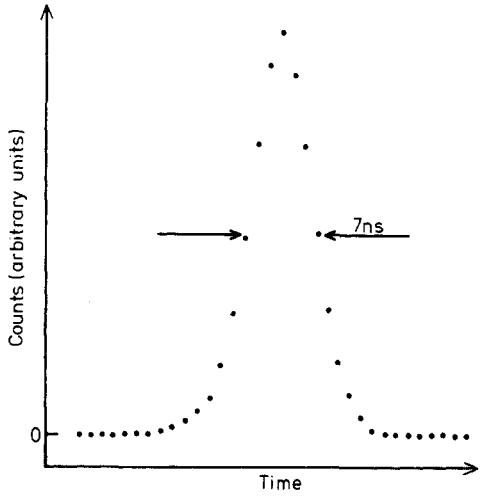

Figure 2. TOF distribution of the 200 eV primary beam bursts. The dots represent count numbers accumulated in the bins of a multichannel analyser.

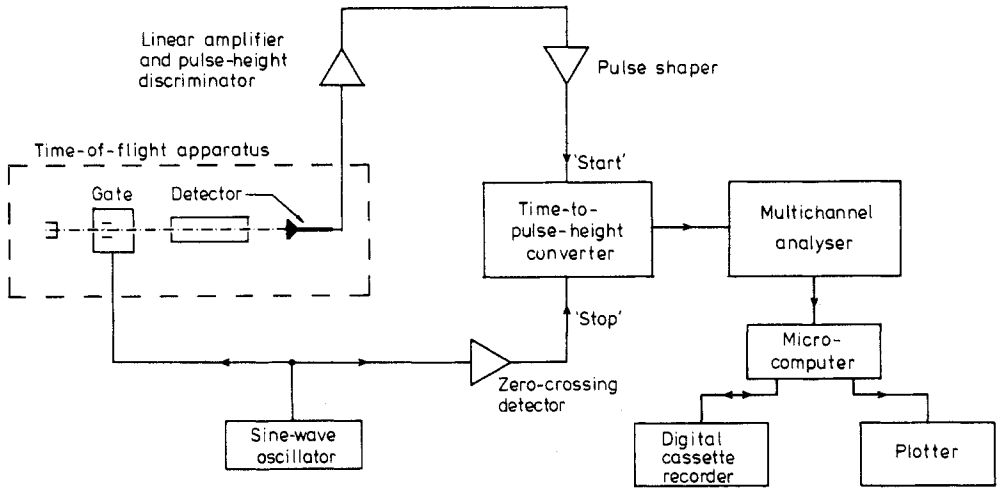

Figure 3. Block diagram of electronic instrumentation.

This corrected flight time, t, is a measure of the electron energy, E. For the sake of simplicity we shall always refer to the measured spectra as distributions of electron-beam intensity as a function of kinetic energy, $I(E)$, although the raw data are actually flight time distributions $I(t)$.

The electron optics employed consist of numerous beam-deflection devices for fine adjustments, some electrostatic lenses and a magnetic lens as well as magnetic deflection coils in the drift-tube region where potential gradients must be avoided.

The gas handling system is shown schematically in figure 4. In the course of a measurement gas is let into the target chamber and into the outer vacuum chamber alternatingly. The gas flux into the apparatus is kept constant so that the equilibrium

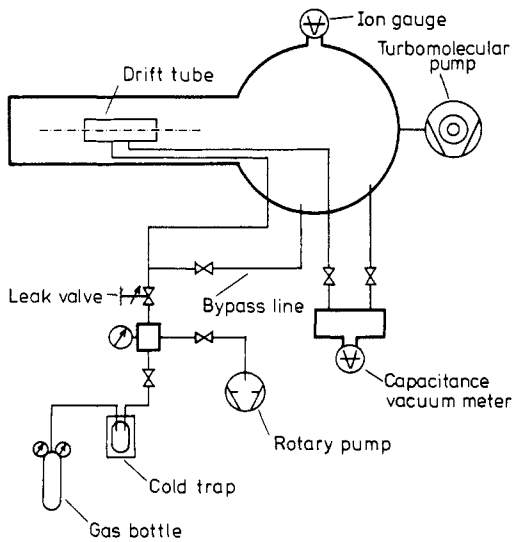

Figure 4. Gas handling system (not to scale).

pressure outside the drift tube is the same in both modes of operation. With a gauge at the end of the arm of the vacuum system (not shown in figure 4) we could not detect any pressure changes when the way of the gas flow was altered, thus the pressure gradient along the arm, outside the drift tube, is negligible. Therefore the cathode and other external structures are always exposed to the same partial pressure of the target gas. The target gas pressure is measured with a capacitance manometer located in a separate chamber which is an extension of the drift tube (cf figure 4). We use an MKS Baratron capacitance manometer with pressure head type 310 BHS-1, bakeable, thermally stabilised at 27 °C which is 1–2 degrees above room temperature. Therefore, thermal transpiration correction is negligible. A few days before the start of the absolute pressure measurements the manometer was recalibrated in our presence at the Munich laboratory of MKS.

The pressure gradient along the drift tube from the gas inlet at the middle to the holes at both ends was estimated. The necessary correction of the target gas pressure is smaller than 0·5%. There are no baffles inside the drift tube, the tube ID is 22 mm. Entrance and exit holes are 2 mm in diameter and the adjacent electrodes (separated only by a thin mica sheet for insulation) have holes with 1 mm diameter.

The ionisation gauge located outside the drift tube in the directly pumped main chamber measures the stationary background pressure. This pressure is the result of an equilibrium between gas input and pumping speed and is proportional to the target gas pressure since the pressure ratio, determined by the size of the electrode apertures at both ends of the drift tube, is constant for a given gas. Thus, the outside ionisation gauge reading the background pressure can be calibrated against the capacitance manometer measuring the target pressure. The calibration factor contains the gauge sensitivity for the given gas as well as the pressure ratio maintained by the differential pumping (which also depends on the gas because of the pumping speed). The use of the calibrated ionisation gauge is advantageous because it responds more quickly than the capacitance manometer which is connected to the target by long and thin tubing.

The pumping system was changed from the formerly used mercury diffusion pump (200 l s^{-1}) with a liquid-nitrogen trap to a turbomolecular pump (250 l s^{-1}) without a trap.

2.2. Procedures

Electron TOF distributions are measured with and without gas in the drift tube. In the mode 'with gas' the electron intensity is attenuated by the scattering in the target. For any given flight time, t, corresponding to the energy, E, the detected intensity 'with gas' and 'without gas', $I(E)$ and $I_0(E)$ respectively, determine the total scattering cross section according to

$$I(E) = I_0(E) \exp(-\sigma(E)nl) \tag{1}$$

where n is the particle density and l the length of the target.

The switch from the mode of measurement 'with gas' to that 'without gas' changes the particle density in the target. If it also causes other changes in the apparatus serious systematic errors can occur. The variation of the cathode temperature, employed in the early work (Land and Raith 1974) to offset the intensity attenuation due to the target gas scattering, introduced slight changes in the general slope of $\sigma(E)$ and precluded the splicing of data sets obtained for adjoining energy intervals. Apparently it also caused false structures under certain circumstances. Later investigations of disturbing effects

showed that the electron beam intensity definitely must remain constant during a measuring cycle. The loss of signal due to target scattering must be suffered and taken into account by a correspondingly longer counting time. This new procedure, together with other measures for increasing the stability of the whole system and improving electronics and electron optics led to a much better performance of the spectrometer. The splicing of data sets is now possible (figure 5).

A mass spectrometer for background gas analysis was added and it was found that it is essential to bake the system until no traces of H_2O can be detected. Otherwise, it is impossible to get electrons of very low energy through the TOF system.

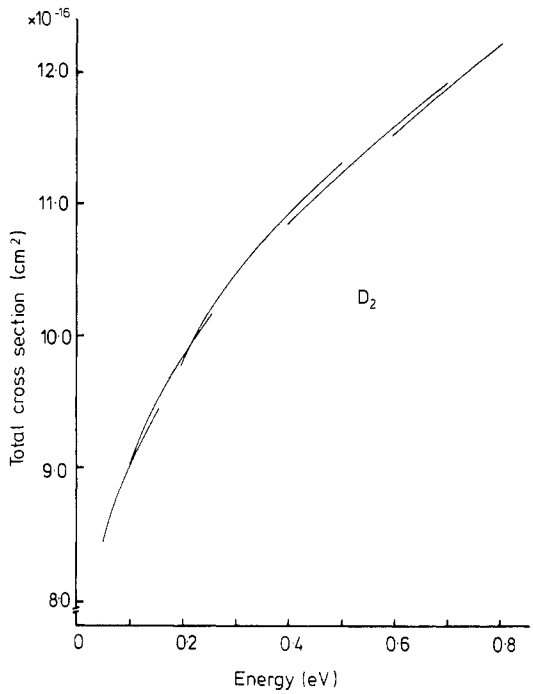

Figure 5. Splicing of data sets here shown for D_2 data.

3. Data taking

First, the apparatus is baked in order to achieve a water-vapour-free pressure of about 2×10^{-8} Torr. The gas flow into the system is started hours before data are taken in order to assure that all surfaces get an equilibrium layer of gas atoms and that work-functions become stabilised. The tuning of the low-energy electron beam traversing the drift tube is a tedious procedure which requires familarity with the system and patience. When the tuning has led to a satisfactory spectrum, the TOF measurement with and without gas in the target, is started. The data accumulation times for both modes of measurement are chosen such that the statistical error of I_0/I is minimised for a given total data-taking time.

The TOF spectra are then processed by the built-in computer of the multichannel analyser (MCA) which leads to the spectrum of $\ln(I_0/I)$ as a function of flight time. The conversion from flight time t to the kinetic energy E as independent variable is done by

an on-line microprocessor which also controls the data output to plotter and tape. The true flight time can be determined from measurements of the time between detection of a given electron and the next zero crossing of the RF sweep, measurements of the corresponding time for 200 eV electrons, and the value of the sweep frequency. The energy computed from that flight time is on an absolute scale.

The energy scale used in plotting the $\sigma(E)$ data has been computed from the measured flight time, t and drift-tube length, l, according to $E = m(l/t)^2/2$. In addition, a small correction has been made in order to account for the fact that the electrons do not change their velocity abruptly when they enter and leave the drift tube. In the region near the entrance and exit aperture the potential changes gradually over several millimeters. With a computer program which solved the Laplace equation for the given electrode configuration and then computed electron trajectories (Herrmannsfeldt 1965), we determined the corrections which amount to a shift of 2–5 meV at low electron energies, depending on the potentials of the electrodes adjacent to the drift tube.

An important criterion for the reliability of the data is given by their reproducibility under a variety of different conditions. At very low electron energies only a small energy interval can be covered with one spectrum $I_0(E)$. In each of those small intervals at least ten measurements are always made with different electron optical settings and, therefore, different spectra $I_0(E)$. The target pressure (the gas flow into the system) is also varied. These ten or more measurements are then averaged by taking the mean of the cross section data at numerous energy values and drawing a curve through those mean values. The stated error bars correspond to two times the Gaussian standard deviation for this averaging. The statistical counting error of any individual measurement is considerably smaller. The systematic error, common to all of our measurements, results mainly from pressure gauge calibration and target length determination; it was estimated to be smaller than 1%.

Another systematic error can possibly result from scattered electrons which do not disappear from the detected beam but are scattered a second time in such way that they can leave the drift tube and reach the detector. In searching for this effect we examined the pressure dependence of the counting rates and tested the beam intensity as a function of the magnetic steering. From the negative results of these tests we concluded that this effect is negligible compared with the other uncertainties in the absolute cross section determination.

The dependence of the measured values of $\ln I_0/I$ on target pressure p was checked repeatedly (figure 6). A linear relation was always found. As Bederson and Kieffer (1971) pointed out this is a necessary but not sufficient condition for obtaining reliable absolute cross section values.

4. Test measurements with helium and oxygen

In order to check the performance of the spectrometer with regard to absolute cross section measurements, we used helium, for which reliable data for comparison exist. From a curve drawn through numerous data points we selected ten values (dots on figure 7) and used them for a least-squares fit to the 'effective-range formula' of O'Malley (1963),

$$\sigma = 4\pi[A^2 + (2\pi/3a_0)\alpha Ak + (8/3a_0)\alpha A^2k^2 \ln(ka_0) + Bk^2 + \dots] \qquad (2)$$

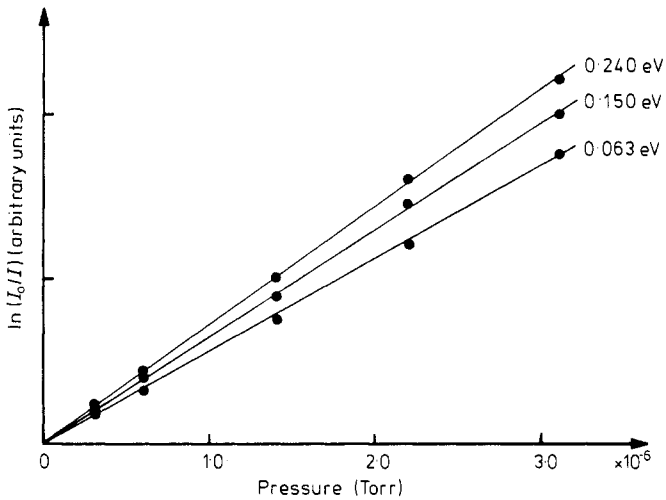

Figure 6. Linearity check: scattering power versus gas pressure (here the target gas is H_2).

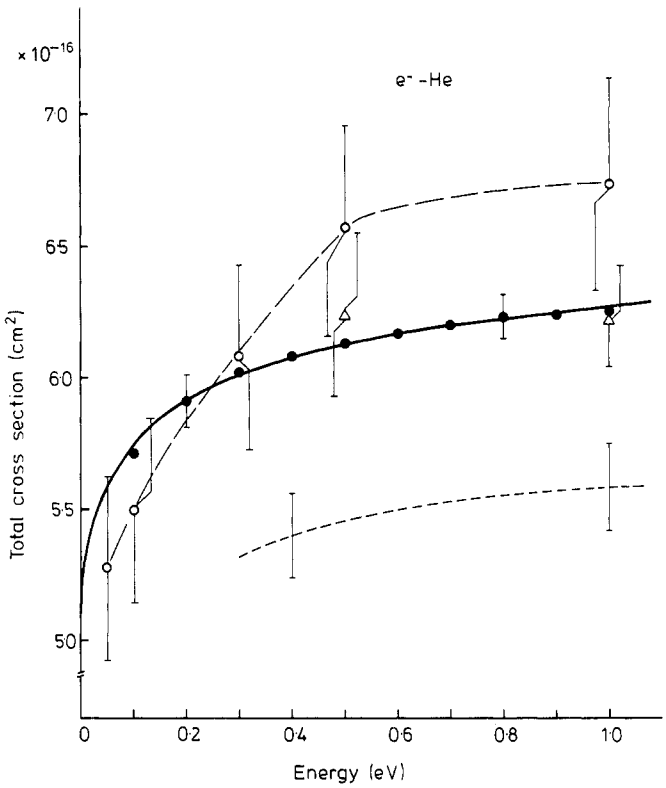

Figure 7. Test for absolute cross section measurements: the full curve is a least-squares fit of our data points (dots) for helium to a theoretical model as explained in the text. Also shown are the experimental results of three other groups. △, Kennerly and Bonham (1978); ○, Gus'kov *et al* (1978); – – –, Golden and Bandel (1965). Our measurements have a statistical error of ±2% (indicated by error bars) and an estimated systematic error of ⩽1%.

with $k^2 = (2m/\hbar^2)\,E$, in which the zero-energy scattering length, A, and the constant, B, are fitting parameters, a_0 is the Bohr radius and $\alpha = 1{\cdot}46a_0^3$ is the tabulated polarisability of helium (Stuart 1950). The fit led to the function shown as the full curve in figure 7. For the zero-energy cross section we obtain $\sigma(0) = 5{\cdot}03 \times 10^{-16}$ cm^2, equivalent to $A = 1{\cdot}195\ a_0$.

In the range of 0·5–1·0 eV where our measurements overlap with those of Kennerly and Bonham (1978) the agreement is very good. The data of Golden and Bandel (1965) show the same energy dependence but lie about 10% below ours. In view of the uncertainties indicated by the error bars the data of Gus'kov *et al* (1978) are consistent with ours but suggest a greater slope of $\sigma(E)$ at very low energies.

Very reliable absolute cross section values come from electron swarm experiments. Although the quantity actually measured in those experiments is the momentum-transfer cross section, σ_m, averaged over a broad energy distribution, it is now possible to obtain $\sigma_m(E)$ by elaborate data evaluation with high-speed computers (cf Gilardini 1972). The most recent and most precise swarm results on helium are those of Crompton *et al* (1970). Their data evaluation yielded $\sigma_m(E)$ values down to $E = 0{\cdot}008$ eV and permitted extrapolation to zero energy. At $E = 0$ the momentum-transfer cross section equals the total cross section according to theory (O'Malley 1963). With $\sigma_m(0) = 4\pi A^2$ Crompton *et al* obtained $A = 1{\cdot}19\ a_0$ in excellent agreement with our extrapolation.

For a comparison with theory we refer to the very recent variational calculations of Nesbet (1979) which predict $A = 1{\cdot}1835\ a_0$ (±0·5%) in satisfactory agreement with our A determination. Agreement exists also at non-zero energies.

The energy resolution of the spectrometer had originally been demonstrated by resolving the fine structure of the low-lying O_2 resonances (Land and Raith 1974). After all the spectrometer modifications had been made we repeated those measurements. The data for the lowest resonance are shown in figure 8 and prove that the alterations did not adversely affect the energy resolution of the spectrometer.

As estimated from design parameters and operation characteristics this spectrometer has an energy resolution of about $\Delta E = 0{\cdot}005$ eV at $E \sim 0{\cdot}250$ eV; above that energy the resolution is limited by the timing error and ΔE increases proportional to $E^{3/2}$. At lower energies the resolution should be even better. For H_2 as target gas the resolution limiting effect below 0·250 eV is the Doppler broadening for which ΔE is proportional to $E^{1/2}$.

Results

A comparison of our data for H_2, D_2 and HD showed no significant differences within the accuracy of the measurements (±2% for H_2 and D_2, ±2·5% for HD). The total cross section increases slowly with energy; no pronounced structures were observed.

In figure 9 our hydrogen data are compared with other results. For our data we claim an accuracy of ±2·5% taking into account statistical as well as systematic errors. The two beam experiments of Ramsauer and Kollath (1930) and Golden *et al* (1966) gave almost identical results for $E \geqslant 0{\cdot}9$ eV. Down at $E \simeq 0{\cdot}2$ eV the cross section of Ramsauer and Kollath lies 16% above ours, that of Golden *et al* 12% below. Of the two theoretical predictions the more recent one of Morrison and Lane (1975) is rather close to our data, particularly at very low energies.

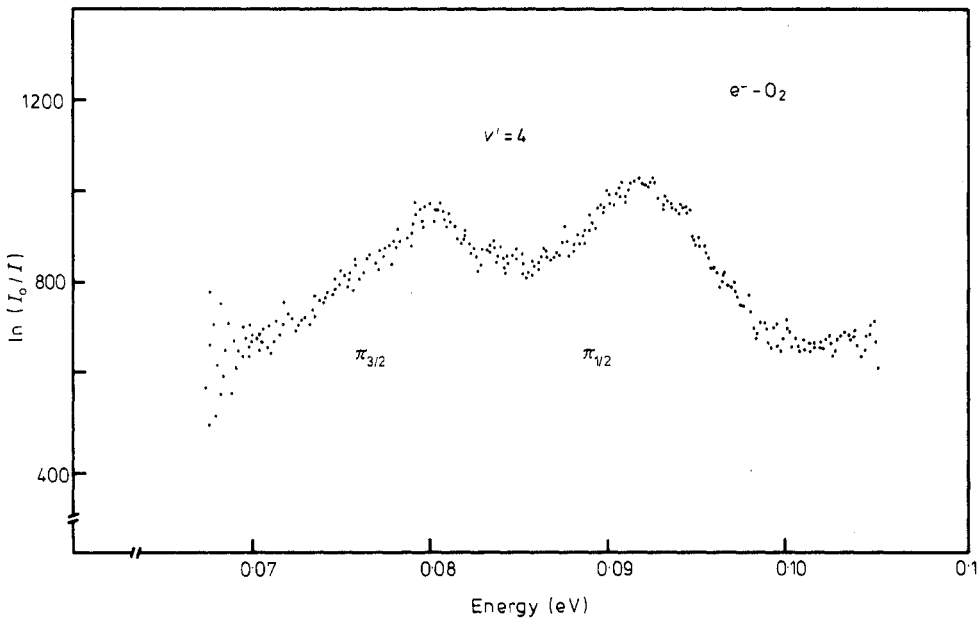

Figure 8. Test of energy resolution: measurements with O_2 near the energy of the lowest lying resonance, corresponding to the vibrationally excited state of O_2^- with quantum number $v' = 4$. The width of the $\pi_{3/2}/\pi_{1/2}$ doublet peaks is not determined by the resolution of the spectrometer but rather by the width of the band which results from a superposition of numerous different rotational transitions associated with this vibrational excitation.

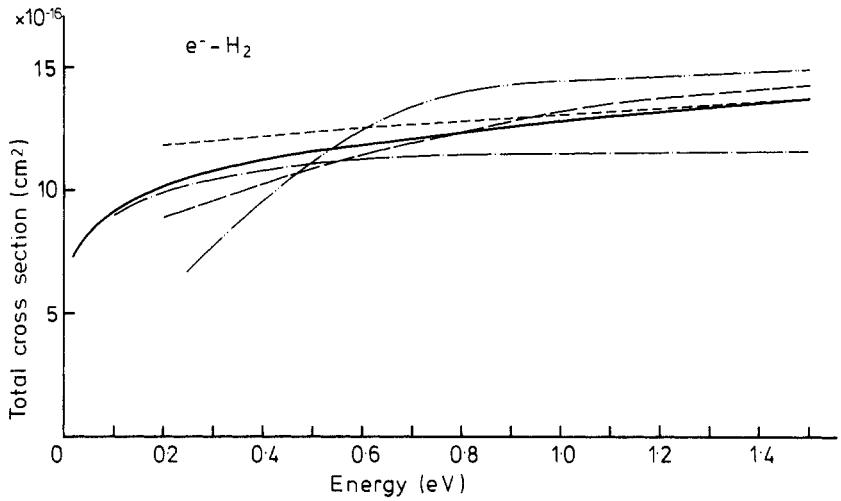

Figure 9. Comparison of our data on molecular hydrogen with other results. Experimental: ------, Ramsauer and Kollath (1930); – – –, Golden *et al* (1966); ——, this work. Theoretical: – · · –, Wilkins and Taylor (1967); – · –, Morrison and Lane (1975).

A direct comparison with results from swarm experiments is not possible since swarm experiments yield the momentum-transfer cross section, $\sigma_m(E)$, which differs from $\sigma(E)$. The use of modified effective range theory for extrapolation to zero energy

is questionable in the case of H_2 as the applicability of this theory has only been demonstrated for the noble gases. The swarm experiments of Crompton *et al* (1969) yielded $\sigma_m(E)$ values which are larger than our $\sigma(E)$ values by 18% at $E = 0{\cdot}04$ eV and 34% at $E = 1{\cdot}3$ eV. This difference between the σ_m and σ measurements is not necessarily a contradiction; more theoretical guidance is needed before a critical comparison can be made.

Acknowledgments

The authors thank Ms S Höwelmann for her assistance in data taking. The cooperation of the machine-shop and electronic-shop staff is gratefully acknowledged. This work has been supported by the University of Bielefeld under Project No 2855.

References

Bederson B and Kieffer L J 1971 *Rev. Mod. Phys.* **43** 601–40
Crompton R W, Elford M T and Robertson A G 1970 *Aust. J. Phys.* **23** 667–81
Crompton R W, Gibson D K and McIntosh A I 1969 *Aust. J. Phys.* **22** 715–31
Crompton R W and Robertson A G 1971 *Aust. J. Phys.* **24** 543–53
Frommhold L 1968 *Phys. Rev.* **172** 118–25
Garrett W R 1977 *Phys. Rev.* A **16** 2305–14
Gilardini A 1972 *Low Energy Collisions in Gases* (New York: Wiley)
Golden D E and Bandel H W 1965 *Phys. Rev.* **138** A14–21
Golden D E, Bandel H W and Salerno J A 1966 *Phys. Rev.* **146** 40–2
Gus'kov Yu K, Savvov R V and Slobodyanyuk V A 1978 *Sov. Phys.-Tech. Phys.* **23** 167–71
Henry R J W and Lane N F 1969 *Phys. Rev.* **183** 221–31
Herrmannsfeldt W B 1965 *Stanford Linear Accelerator Center, SLAC Report* No 51
Kennerly R E and Bonham R A 1978 *Phys. Rev.* A **17** 1844–54
Kouri D J, Sams W N and Frommhold L 1969 *Phys. Rev.* **184** 252–4
Land J E and Raith W 1973 *Atomic Physics 3* ed S J Smith and G K Walters (New York: Plenum) p 553–9
—— 1974 *Phys. Rev.* A **9** 1592–602
Matsuzawa M 1975 *J. Phys. B: Atom. Molec. Phys.* **8** L382–6
Morrison M A and Lane N F 1975 *Phys. Rev.* A **12** 2361–8
O'Malley T F 1963 *Phys. Rev.* **130** 1020–9
Nesbet R K 1979 *Phys. Rev.* A **20** 58–70
Ramsauer C and Kollath R 1930 *Ann. Phys. Lpz.* (5) **4** 91–108
Stuart H 1950 *Landolt-Börnstein* vol 1, ed A Eucken (Berlin: Springer) pp 399–404
Taylor H S and Harris F E 1963 *J. Chem. Phys.* **39** 1012–6
Wilkins R L and Taylor H S 1967 *J. Chem. Phys.* **47** 3532–9